Subunit D of RNA polymerase from *Methanosarcina acetivorans* contains two oxygen-labile [4Fe-4S] clusters: implications for oxidant-dependent regulation of transcription *

Faith H. Lessner[1], Matthew E. Jennings[1], Akira Hirata[2], Eduardus C. Duin[3], and Daniel J. Lessner[1]

[1]From the Department of Biological Sciences, University of Arkansas-Fayetteville, Fayetteville, AR, 72701
[2]Department of Materials Science and Biotechnology, Ehime University, Matusyama, Japan
[3]Department of Chemistry and Biochemistry, Auburn University, Auburn, Alabama, 36849

*Running title: *2[4Fe-4S] cluster-containing RNA polymerase*

To whom correspondence should be addressed: Daniel J. Lessner, Department of Biological Sciences, University of Arkansas, Fayetteville, AR, USA, Tel.: (479) 575-2239; Fax: (479) 575-4010; E-mail: dlessner@uark.edu

Background: RNAP from several species of *Archaea* and *Eukarya* is predicted to contain Fe-S clusters.

Results: We show here that Subunit D of RNAP from *M. acetivorans* contains two redox-active and oxygen-labile [4Fe-4S] clusters.

Conclusion: The [4Fe-4S] clusters are not required for D/L heterodimer formation, but affect the stability of the heterodimer.

Significance: The [4Fe-4S] clusters may regulate the assembly and activity of RNAP in an oxidant – dependent manner.

SUMMARY

Subunit D of multi-subunit RNA polymerase (RNAP) from many species of Archaea is predicted to bind one to two iron-sulfur (Fe-S) clusters, the function of which is unknown. A survey of encoded subunit D in the genomes of sequenced Archaea revealed six distinct groups based on the number of complete or partial [4Fe-4S] cluster motifs within domain 3. Only the subunits D from strictly anaerobic Archaea, including all members of the *Methanosarcinales*, are predicted to bind two [4Fe-4S] clusters. We report herein the purification and characterization of *Methanosarcina acetivorans* subunit D in complex with subunit L. Expression of subunit D and subunit L in *Escherichia coli* resulted in the purification of a D/L heterodimer with only partial [4Fe-4S] cluster content. Reconstitution *in vitro* with iron and sulfide revealed that the *M. acetivorans* D/L heterodimer is capable of binding two redox-active [4Fe-4S] clusters. *M. acetivorans* subunit D deleted of Domain 3 (DΔD3) was still capable of co-purifying with subunit L, but was devoid of [4Fe-4S] clusters. Affinity-purification of subunit D or subunit DΔD3 from *M. acetivorans* resulted in the co-purification of endogenous subunit L with each tagged subunit D. Overall, these results suggest that Domain 3 of subunit D is required for [4Fe-4S] cluster binding, but the [4Fe-4S] clusters and domain 3 are not required for the formation of the D/L heterodimer. However, exposure of 2[4Fe-4S] cluster containing D/L heterodimer to oxygen resulted in loss of the [4Fe-4S] clusters and subsequent protein aggregation, indicating that the [4Fe-4S] clusters influence the stability of the D/L heterodimer and therefore have the potential to regulate the assembly and/or activity of RNAP in an oxidant-dependent manner.

1

DNA-dependent RNA polymerase (RNAP) is a multi-subunit enzyme that is essential in all cellular organisms, where it acts in concert with a vast array of gene-specific activators, repressors, and general transcription factors to modulate the synthesis of RNA. The core catalytic component of RNAP is conserved in all three domains of life (*Bacteria, Archaea,* and *Eukarya*). The diversity in RNAPs lies in the number of RNAP complexes and their subunit composition. Eukaryotes have three separate nuclear RNAPs (Pol I, II, and III) that transcribe non-overlapping subsets of genes (1,2). Each eukaryotic RNAP contains at least 10 subunits. In addition to the three RNAPs, higher plants possess Pol IV (NRPD1) and Pol V (NRPE1) that transcribe non-coding RNAs involved in RNA silencing (3). *Archaea* and *Bacteria* contain a single RNAP that transcribes all genes. Bacterial RNAP is the least complex, containing only the core component comprised of five subunits ($\alpha_2\beta\beta'\omega$). Archaeal RNAP consists of 12-13 subunits (RpoA-P) depending on phyla, similar to the subunit composition of eukaryotic RNAPs. Archaeal RNAP is most similar to eukaryotic Pol II, which consists of 12 subunits (Rpb1-12). The similarities between archaeal and eukaryotic RNAP were confirmed following the recent elucidation of the structures of archaeal RNAP (4-6). One of the more striking features of the *Sulfolobus solfataricus* RNAP structure was the presence of an iron-sulfur (Fe-S) cluster in subunit D. Fe-S clusters are cofactors typically found in metabolic enzymes where they function in the transfer of electrons, but also have catalytic, sensing and structural roles (7). The function of Fe-S cluster(s) in RNAP is unknown.

Subunit D of archaeal RNAP contains three domains. Domains 1 and 2 are conserved in the homologous Rpb3 subunit of Pol II, AC40 subunit of Pol I/III, and bacterial α subunit (8). Domain 1 is divided into three regions and is involved in dimerization with subunit L (RpoL), the initial step in the assembly of RNAP (9,10). Domain 2 is involved in the interaction with additional RNAP subunits and general transcription factors. Domain 2 of *S. solfataricus* subunit D contains four cysteines that form two intramolecular disulfides (4). However, these cysteines are not conserved in all RpoD/Rpb3/AC40/α subunits, and the four cysteines of domain 2 in yeast Rpb3 chelate a zinc ion (11). Domain 3 of *S. solfataricus* subunit D contains six cysteine residues, four of which are found in a typical [4Fe-4S] cluster binding motif. The structure of the D/L heterodimer from *S. solfataricus* revealed a [3Fe-4S] cluster present in domain 3 of subunit D, ligated by C183, C203, and C209 (4). The cluster is likely a [4Fe-4S] cluster *in vivo*, with C206 serving as the fourth ligand. The two remaining cysteines of domain 3 form an intramolecular disulfide. The [4Fe-4S] cluster binding motif is not restricted to *S. solfataricus* subunit D, but is found in D and Rpb3/AC40 subunits in various species of *Archaea* and *Eukarya*. However, all bacterial α subunits lack the residues of domain 3 and therefore are not predicted to bind Fe-S clusters (8).

Previous phylogenetic analysis indicated that there are four groups of archaeal D subunits based on the number of complete [4Fe-4S] cluster binding motifs in domain 3 (8). A re-examination here of the cysteine content in subunit D domain 3 encoded in the genomes of sequenced Archaea in the NCBI database (NCBI) indicates the classification should be expanded to six distinct groups based on complete or partial [4Fe-4S] cluster motifs (see results). Conservation of the [4Fe-4S] cluster binding motif(s) in RNAP in multiple archaeal lineages and in some eukaryotes suggests that the clusters serve an important role(s). The Fe-S clusters have been postulated to function in regulation of the *de novo* assembly of RNAP, in which the presence of the cluster(s) is required for the formation of the D/L heterodimer (8), the first step in the assembly of RNAP in archaea.

Only strictly anaerobic archaea contain RNAP subunit D with two [4Fe-4S] cluster motifs. However, not every anaerobic archaeon possesses a RNAP subunit D with [4Fe-4S] cluster motifs. For example, all methane-producing archaea (methanogens) are strict anaerobes, yet there is extensive diversity in the properties of domain 3 of subunit D. Moreover, the ability of subunit D to bind two [4Fe-4S] clusters has not been documented. We report herein that subunit D from the methanogen *Methanosarcina acetivorans* binds two [4Fe-4S] clusters, consistent with the presence of two

[4Fe-4S] cluster binding motifs, and that the clusters are similar to the [4Fe-4S] clusters in ferredoxin. Expression studies combined with mutational analysis also demonstrate that although domain 3 of subunit D is required for [4Fe-4S] cluster binding, the [4Fe-4S] clusters and amino acid residues of domain 3 are not required for the initial association of subunit D with subunit L. However, the [4Fe-4S] clusters are oxygen-labile, and oxygen-dependent loss of the [4Fe-4S] clusters impacts the structural stability of the D/L heterodimer. Implications for the regulation of RNAP assembly and activity by the [4Fe-4S] clusters in methanogens are presented.

EXPERIMENTAL PROCEDURES

Homology model of the M. acetivorans D/L heterodimer- A structural model of the D/L heterodimer from *M. acetivorans* was generated by SWISS-MODEL (12). The PDB coordinates of the *Sulfolobus solfataricus* D/L heterodimer (PDB ID: 2PA8) and ferredoxin-like domain of *Archaeoglobus fulgidus* adenylylsulfate reductase (PDB ID: 1JNR) were used as templates for the generation of the structural model. The model generated for domain 3 including the two [4Fe-4S] clusters was manually traced onto domain 3 of the *Sulfolobus solfataricus* structure by COOT (13).

Plasmid construction and mutagenesis- For co-expression of *M. acetivorans* subunits D (RpoD) and L (RpoL) in *E. coli*, the plasmid pMaRpoDL was constructed. Primers were used to amplify *rpoL* from *M. acetivorans* C2A genomic DNA resulting in a product with *Nde*I and *Xho*I sites at the 5' and 3' ends, respectively. The PCR product was digested with *Nde*I and *Xho*I and ligated to pET21a that had been similarly digested. The resulting plasmid (pMaRpoL) contained *rpoL* fused with a C-terminal six-histidine tag (His tag) under the control of the T7 promoter. The gene encoding *rpoD* was amplified from *M. acetivorans* C2A genomic DNA using a forward primer with a *Nde*I site and a reverse primer containing a *Bam*HI site. The PCR product was digested with *Nde*I and *Bam*HI and ligated with pET21a that was digested with the same enzymes. The resultant plasmid, pMaRpoD, contained an untagged *rpoD* gene under the control of the T7

promoter. pMaRpoD was digested with *Bgl*II and *Bam*HI. The roughly 1 kb fragment containing the T7 promoter and *rpoD* was gel-extracted, purified, and ligated with *Bgl*II-digested pMaRpoL, creating the pMaRpoDL plasmid. pMaRpoDL contains both *rpoD* and *rpoL*, each regulated by a separate T7 promoter. Importantly, only subunit L contains a His tag, designated subunit L(his). *E. coli* DH5α was used as the parent strain for all manipulations and was grown in Luria broth or agar containing appropriate antibiotics at 37 °C.

PCR amplification was used to remove the domain 3 amino acid residues 171 to 221 from *M. acetivorans* subunit D, the region which encompasses both [4Fe-4S] cluster motifs. Primers RpoDFeS2KORev (5'- AAT GGT AAT TAC AGG CAT GTT TTT G -3') and RpoDFeS1KOFor (5'- GTG GAC TTC TAT GAA AAC TCT TTT G -3') were 5'-phosphorylated and used to amplify pMaRpoDL minus domain 3 of subunit D. The ends of the amplified product were blunt-ligated forming pDL408. In-frame deletion of the codons encoding amino acid residues 171-221 of subunit D was confirmed by DNA sequencing. Subunit D harboring the deletion was designated subunit DΔD3. Plasmid pDL408 was used for co-expression of subunit DΔD3 with subunit L(his).

Expression and purification of recombinant M. acetivorans D/L heterodimer- All recombinant proteins were expressed in *E. coli* Rosetta (DE3) (pLacI) cells containing pRKISC, which increases the level of iron-sulfur cluster biogenesis proteins (14). Unless stated otherwise, cells were grown in Terrific broth containing 50 µg/ml ampicillin, 17 µg/ml chloramphenicol, and 5 µg/ml tetracycline at 37 °C with shaking at 250 rpm. Once an optical density at 600 nm of 0.5 to 0.7 was reached, the growth temperature was adjusted to 25 °C, 0.2 mM ferrous ammonium sulfate was added to the medium, and the culture was induced with the addition of 0.5 mM isopropyl-β-D-thiogalactopyranoside (IPTG). The cells were harvested by centrifugation 16 h after induction.

All subsequent purification procedures were performed anaerobically within an anaerobic chamber (Coy Laboratory Products)

3

containing an atmosphere of 95% N_2 and 5% H_2. Approximately 10 g of cells was suspended in 35 ml of 20 mM Tris-HCl (pH 8) containing 500 mM NaCl, 2 mM benzamidine, and a few crystals of DNaseI. The cells were lysed by two passages through a French pressure cell at over 110 Mpa. The lysate was centrifuged at 70,000 x *g* for 35 min at 4 °C. The supernatant containing the expressed protein(s) was filtered (pore size, 0.45 μm) and applied at a flow rate of 0.5 ml min^{-1} to a column containing 5 ml of Ni^{2+}-agarose resin (Genscript). The column was then washed with 25 ml of 20 mM Tris-HCl (pH 8), 500 mM NaCl, followed by a 25 ml wash with the same buffer containing 10 mM imidazole. Bound protein(s) were eluted from the column by the addition of 15 ml of 20 mM Tris-HCl (pH 8), 500 mM NaCl containing 250 mM imidazole. The eluate was concentrated using a Vivacell concentrator (Sartorius) with a 10,000-molecular-weight cutoff under nitrogen flow inside the anaerobic chamber. The concentrated protein was desalted into 50 mM HEPES (pH 7.5) containing 150 mM NaCl using a PD-10 column (GE Healthcare). The desalted protein was either frozen under N_2 at -80 °C or immediately processed by size-exclusion chromatography.

Size-exclusion chromatography was performed using a Sephacryl HiPrep S-200 gel filtration fast protein liquid chromatography column (GE Healthcare) with a Biologic LP system (Biorad) within an anaerobic chamber. Samples were analyzed with a running buffer of 50 mM HEPES (pH 7.5) containing 150 mM NaCl and 2 mM DTT at a flow rate of 0.5 ml min^{-1}. The column was calibrated with the following proteins having known molecular masses: β-amylase (200 kDa), alcohol dehydrogenase (150 kDa), bovine serum albumin (66 kDa), carbonic anhydrase (29 kDa), and cytochrome *c* (12.4 kDa). Samples (2 ml) containing 50-75 mg of total protein were loaded onto the column per run.

D/L(his) proteins were reconstituted with iron and sulfide similar to as described (15). All additions and incubations were done under anaerobic conditions at 4 °C. Briefly, the eluate containing subunit D and subunit L(his) from the Ni^{2+}-agarose resin was concentrated and desalted into 50 mM Tris-HCl (pH 8.0).

Approximately 50 mg of total protein was diluted in 50 ml of 50 mM Tris-HCl pH 8.0 containing 2 mM β-mercaptoethanol in a 125 ml serum bottle. After 30 minutes, ferrous ammonium sulfate was added drop-wise to a final concentration of 120 mM. After another incubation of 30 minutes, sodium sulfide was added drop-wise to a final concentration of 120 mM. The protein/iron/sulfide mixture was incubated for 16 h at 4 °C. The protein was then concentrated using a stirred cell concentrator (Millipore) with a 10,000-molecular weight cutoff and subsequently desalted into 50 mM HEPES pH 7.5 containing 150 mM NaCl and analyzed by size-exclusion chromatography.

Analytical methods- Protein concentrations were determined by the method of Bradford using bovine serum albumin as a standard (16). The concentration of the D/L(his) heterodimer was also determined using the calculated extinction coefficient at 280 nm of 21,890 mM^{-1} cm^{-1}. The results from both methods were in good agreement (< 5% deviation). The iron and acid-labile sulfide content of D/L(his) heterodimers was determined as previously described (17). The number of thiols in D/L(his) heterodimers was determined using Ellman's reagent (dithionitrobenzoate, DTNB) (18). In brief, thiol measurements were performed in 100 mM phosphate buffer (pH 8) with 0.2 mM DTNB in both the presence and absence of 6 M guanidine hydrochloride. The absorbance at 412 nm was measured after room temperature incubation for 15 minutes. An extinction coefficient at 412 nm of 14,150 mM^{-1} cm^{-1} and 13,700 mM^{-1} cm^{-1} was used for sulfhydryl content determination in buffer or buffer containing guanidine hydrochloride, respectively. Mass spectrometry of purified proteins was performed at the University of Arkansas Statewide Mass Spectrometry facility (Fayetteville, AR). SDS-PAGE and Western blotting were performed by standard procedures. The anti-RpoDL antibody was raised in rabbit against recombinantly-purified D/L(his) heterodimer.

CW electron paramagnetic resonance (EPR) spectra were measure at X-band (9 GHz) frequency on a Bruker EMX spectrometer, fitted with the ER-4119-HS high sensitivity perpendicular-mode cavity. General EPR

conditions were: microwave frequency, 9.385 GHz; field modulation frequency, 100 kHz; field modulation amplitude, 0.6 mT. Sample specific conditions are indicated in the figure legends.

Cloning, expression, and purification of subunit D and DΔD3 with a N-terminal His-tag in M. acetivorans- PCR was used to amplify *rpoD* from *M. acetivorans* C2A genomic DNA. The forward primer for the amplification contained the sequence for an *Nde*I restriction site and an N-terminal His-tag (5'- ATT AAG GCA TAT GCA TCA TCA TCA TCA TCA TAC GAT GGA AGT AGA CAT TCT -3'), while the reverse primer contained a *Hind*III restriction site (5'- GGT GGT AAG CTT TCA GAG CTG GTC CAG AAT TGC -3'). The PCR product was digested with *Nde*I and *Hind*III and ligated with similarly digested pJK027A (19). The resulting plasmid was named pDL516. To construct a similar plasmid carrying the RpoDΔD3 deletion, the same procedure listed here was performed, only using pDL408 as a PCR template, with the resulting plasmid named pDL409.

M. acetivorans strain WWM73 was transformed with pDL516 and pDL409 as previously described (20). Successful integration of the plasmid was determined as described (19), and the resulting strains named DJL30 (His-D) and DJL31 (His-DΔD3). These strains allow for the tetracycline-regulated chromosomal expression of His-D or His-DΔD3. Cultures of DJL30 or DJL31 were grown anaerobically in HS medium (21) supplemented with methanol and sodium sulfide in the presence and absence of 100 μg/ml tetracycline at 37 °C. The cells were harvested by centrifugation at an optical density at 600 nm of 0.6 under anaerobic conditions.

All purification steps were performed in an anaerobic environment using either, lysis buffer (10 mM Tris-HCl (pH 8), 1 M KCl, 10 μM $ZnCl_2$, 10 mM imidazole, 15% glycerol), wash buffer (10 mM Tris-HCl (pH 8), 0.1 M KCl, 10 μM $ZnCl_2$, 10 mM imidazole, 15% glycerol) or elution buffer (10 mM Tris-HCl (pH 8), 0.1 M KCl, 10 μM $ZnCl_2$, 200 mM imidazole, 15% glycerol). Cell pellets were thawed and suspended on ice in lysis buffer supplemented with a few crystals of DNaseI and benzamidine-HCl. Cells were lysed by sonication, and clarified lysates were obtained after a 35 minute centrifugation step at 70,000 x *g* at 4 °C. The soluble fraction was passed through a 0.45 μm filter and slowly loaded onto a Ni^{2+}-agarose column pre-equilibrated with lysis buffer. The column was washed with 10 column volumes (CV) of lysis buffer followed by 20 CV of wash buffer. Protein was eluted from the column with the addition of 3 CV of elution buffer. Eluates were stored anaerobically in sealed vials at -80 °C.

RESULTS

Archaeal RNAP subunit D classification and diversity of methanogen subunit D- A survey of RNAP D subunits from the ninety-nine sequenced archaeal genomes currently in the NCBI database reveals six distinct groups based on the absent, complete, or partial [4Fe-4S] cluster motifs of domain 3. The domain organization and cysteine residue content of a representative subunit D from each group is shown in figure 1, with *S. solfataricus* subunit D shown as a reference. A complete list of subunit D from individual species and their grouping is listed in Table S1. Briefly, Group 1, complete [4Fe-4S] cluster #1 and #2 motifs (restricted to strict anaerobes); Group 2, a complete [4Fe-4S] cluster #1 motif; Group 3, a complete [4Fe-4S] cluster #2 motif; Group 4, partial [4Fe-4S] cluster #1 and/or #2 motifs; Group 5, absence of [4Fe-4S] cluster motif cysteines; Group 6, lack the amino acid residues of domain 3 (only *Methanococcales*). The corresponding subunit Rpb3 in Pol II or AC40 Pol I/III in certain eukaryotes contain only [4Fe-4S] cluster binding motif #1 and therefore fall in archaeal group 2.

All members of an order typically encode a subunit D within the same group, indicating the presence or absence of the clusters is correlated with particular taxonomic lineages. For example, all Halobacteriales encode a group 5 subunit D, one that is devoid of any cysteine residues. Interestingly, group 1 subunit D is found only in strictly anaerobic Archaea, but is not a universal feature of strict anaerobes. For example, all methanogenic archaea are strict anaerobes and are only capable of growth by methanogenesis using a limited number of substrates, including acetate, H_2/CO_2, and methylated compounds (22). However, despite

the uniform mode of growth and nutritional requirements, there is extensive diversity in the cysteine residue content of subunit D, in particular the number of [4Fe-4S] cluster motifs (Fig. 1S). Subunit D from all sequenced methanogens, except for members of the *Methanococcales*, contains four cysteines in domain 2. Members of *Methanosarcinales*, *Methanomicrobiales*, and *Methanobacteriales* encode subunit D that contains one cysteine residue in domain 1. The majority of methanogens encode subunit D with a domain 3 predicted to bind at least one [4Fe-4S] cluster. All members of the *Methanosarcinales* and *Methanomicrobiales* encode a group 1 subunit D, while members of *Methanobacteriales* encode a group 1 or 2 subunit D. All species of the *Methanococcales* encode subunit D which lacks the amino acid residues of domain 3 and are the only members of group 6. The sole species of *Methanopyrales* encodes a group 4 subunit D. Thus, methanogens provide a unique opportunity to examine the effect of the presence or absence of the [4Fe-4S] clusters within a single group of organisms and correlate results obtained with the metabolism and environment of particular species.

Homology model of the group 1 subunit D from Methanosarcina acetivorans in complex with subunit L- The genome of *M. acetivorans* contains a single *rpoD* gene encoding a 266 amino acid protein with 32% identity to the 265 amino acid subunit D from *S. solfataricus*. However, in the original annotation of the *M. acetivorans* genome, *rpoD* was incorrectly identified as two separate genes (NTO2MA1356-7) (23). Based on the X-ray crystal structure of the *S. solfataricus* D/L heterodimer (4), a homology model of the *M. acetivorans* subunit D in complex with subunit L was generated (Fig. 2).

Similar to *S. solfataricus* subunit D, *M. acetivorans* subunit D contains three domains (Fig. 2A). There are however differences in the cysteine content of each domain between *S. solfataricus* and *M. acetivorans* D subunits. Domain 1 makes up the dimerization interface with subunit L. *M. acetivorans* subunit D contains a single cysteine residue (C160) in domain 1, unlike that of *S. solfataricus*. Domain 2 of *M. acetivorans* subunit D contains four

cysteine residues similar to *S. solfataricus*; however, there is a difference in the spacing of the cysteines. Domain 3 of *M. acetivorans* subunit D contains eight cysteine residues that comprise the two [4Fe-4S] cluster motifs (Group 1 subunit D), whereas domain 3 of *S. solfataricus* subunit D contains six cysteines (Group 2 subunit D). Moreover, a 50-amino acid region of *M. acetivorans* subunit D domain 3 (residues 171-221) has 39% identity to the predicted 60-amino acid 2[4Fe-4S] ferredoxin encoded by *ma0431* in the *M. acetivorans* genome (Fig. 2A). Based on the homology model of the *M. acetivorans* D/L heterodimer, neither domain 2 nor domain 3 is in contact with subunit L, indicating they are likely unnecessary for dimerization with subunit L. In addition, all members of the *Methanoccocales* completely lack the amino acid residues of domain 3, suggesting that domain 3 is likely not necessary for dimerization with subunit L in methanogens.

Expression and purification of recombinant M. acetivorans D/L heterodimer- To determine the capacity of *M. acetivorans* subunit D to bind Fe-S clusters and whether the clusters are required for the interaction and stable association of subunit D with subunit L, each subunit was separately expressed with a C-terminal six-histidine (his) tag in *E. coli*. Subunit L(his) expressed in aerobically-grown *E. coli* was found in the soluble fraction of cell lysates and was purified to homogeneity using Ni^{2+}-affinity and size-exclusion chromatography (data not shown). However, subunit D(his) expressed in aerobically-grown *E. coli* was found only in inclusion bodies in the insoluble fraction of cell lysates. Expression of untagged subunit D or subunit D with a glutathione-S-transferase (GST) tag also resulted in the formation of inclusion bodies (data not shown). The formation of inclusion bodies indicates that subunit D is improperly folded, potentially as a result of the absence of subunit L or incomplete Fe-S cluster incorporation. The lack of Fe-S clusters incorporated into subunit D may be a result of limiting cellular levels of iron, sulfur, or iron-sulfur biogenesis machinery during protein expression in *E. coli*. However, subunit D expressed in anaerobically-grown *E. coli* containing pRKISC, which encodes iron-sulfur cluster biogenesis proteins and has been shown

6

to increase the cluster-content in recombinant Fe-S proteins (24), combined with the addition of supplemental iron, still resulted in the protein being found in insoluble inclusion bodies (data not shown).

Subunit D was subsequently co-expressed with subunit L(his) in aerobically-grown *E. coli*. Size-exclusion chromatography and SDS-PAGE analyses of imidazole-eluted protein from the Ni^{2+}-agarose loaded with cell lysate from *E. coli* co-expressing subunit D and subunit L(his) revealed that subunit D co-purifies with subunit L(his) (Fig. 3A). Three major peaks were detected, all of which contained subunit D and/or subunit L(his). Based on the elution profile of known molecular weight standards, the elution volume of Peak 1 is consistent with D/L(his) complexes larger than a heterodimer ($M_r > 45$ kDa). The elution volume of Peak 3 is consistent with the molecular weight of subunit L(his) ($M_r = 11.1$ kDa). The elution volume of the major Peak (#2) is consistent with a heterodimer of D/L(his) ($M_r = 40.1$ kDa). The presence of higher molecular weight D/L(his) complexes, as well as subunit L(his) monomers, may be a result of differences in expression levels of subunit D and subunit L(his). Co-purification of untagged subunit D with subunit L(his), combined with the insolubility of subunit D in the absence of subunit L under the same conditions, indicates that subunit D is likely unstable or improperly folded when not associated with subunit L.

Purified D/L(his) heterodimer was red-brown in color, indicative of the presence of a chromophore. The UV-visible spectrum of the D/L(his) heterodimer contained absorbance maxima centered at 320 nm and 390 nm, in addition to 280 nm (Fig. 4), consistent with the presence of Fe-S clusters (25). Although *M. acetivorans* subunit D is predicted to contain two [4Fe-4S] clusters, the A_{390}/A_{280} ratio is low, and the experimentally-determined iron and acid-labile sulfide content of as-purified D/L(his) heterodimer is substantially less than predicted (Table 1). The ability to purify D/L(his) heterodimer, which lacks two [4Fe-4S] clusters indicates that the presence of both clusters is not required for the interaction and dimerization of *M. acetivorans* subunit D with subunit L. Attempts to increase the cluster content by co-expression of subunit D with subunit L(his) in anaerobically-grown *E. coli* containing pRKISC and supplementation of the medium with iron did not significantly increase the cluster content of as-purified D/L(his) heterodimer (data not shown).

Reconstitution of [4Fe-4S] clusters in recombinant M. acetivorans D/L(his) heterodimer- To determine the full capacity and type of Fe-S clusters within *M. acetivorans* subunit D, *in vitro* reconstitution of the eluate from the Ni^{2+}-agarose column containing a mixture of subunit D and subunit L(his) was performed by incubation with iron and sulfide as previously described (15). The elution profile from size-exclusion chromatography of the Fe/S-reconstituted sample was identical to that of the non-reconstituted sample (Fig. 3). However, the major peak (#2) corresponding to the D/L(his) heterodimer was of greater intensity than that of non-reconstituted D/L(his) heterodimer, despite loading a similar amount of protein onto the column. The fractions containing peak #2 from the Fe/S-reconstituted sample were dark-brown in color, indicative of increased Fe-S cluster content. These fractions were collected and concentrated, and the sample was designated as the D/L(his)-FeS heterodimer. The D/L(his)-FeS heterodimer had a substantial increase in the A_{390}/A_{280} ratio and extinction coefficient at 390 nm compared to the D/L(his) heterodimer (Table 1), consistent with an increase in Fe-S cluster content. Additionally, compared to the non-reconstituted D/L(his) heterodimer, the D/L(his)-FeS heterodimer contained eight-times the amount of iron and acid-labile sulfide (Table 1), consistent with the incorporation of two [4Fe-4S] clusters into subunit D. Importantly, this experimental protocol is reproducible, as additional preparations of Fe/S-reconstituted D/L(his) heterodimer had similar levels of iron and acid-labile sulfide (data not shown). These data support that *M. acetivorans* subunit D coordinates two [4Fe-4S] clusters.

The D/L(his)-FeS heterodimer showed a broad absorption band centered around 390 nm and a second peak centered around 300 nm, similar to the non-reconstituted heterodimer (Fig. 4). The similarity of domain 3 of *M. acetivorans* subunit D to 2[4Fe-4S] ferredoxin,

7

which functions in electron transfer (26,27), indicates that the [4Fe-4S] clusters in subunit D may have the capacity to participate in oxidation-reduction reactions. The addition of the reductant dithionite to the D/L(his)-FeS heterodimer under anaerobic conditions resulted in a decrease of the absorption band at 390 nm, consistent with reduction of the clusters. EPR spectroscopic analyses of the D/L(his)-FeS heterodimer in the absence of reductant did not reveal any significant signals (Fig. 5). The lack of a $g = 2.01$ EPR signal under these conditions indicates that the D/L(his)-FeS heterodimer does not contain $[3Fe-4S]^+$ clusters, which is consistent with the elemental analyses (Table 1). Addition of dithionite to the sample of D/L(his)-FeS resulted in the appearance of EPR signals with g values at 2.075, 1.974, 1.938, and 1.897 (Fig. 5). The complex $g_{av} = 1.94$ is consistent with the presence of two $[4Fe-4S]^+$ clusters, as is seen with ferredoxins harboring two spin-coupled [4Fe-4S] clusters (28,29). The complexity is caused by spin-spin coupling of the two clusters in close vicinity of each other. Taken together these results support that the D/L(his)-FeS heterodimer contains two redox-coupled $[4Fe-4S]^{2+/+}$ that can possibly participate in one-electron transfers. EPR spectroscopic analyses of the non-reconstituted D/L(his) heterodimer did not produce an EPR signal in the as-purified state or after the addition of dithionite, which may be attributed to insufficient cluster in the samples analyzed. Attempts to obtain more concentrated samples of non-reconstituted D/L(his) for EPR analysis resulted in the precipitation of the protein (data not shown).

Domain 3 of subunit D is required for [4Fe-4S] cluster binding, but is not required for interaction with subunit L-To determine if domain 3 of subunit D is required for [4Fe-4S] cluster binding and dimerization with subunit L, a variant of subunit D deleted of amino acid residues 171 to 221 (Domain 3) was generated. This variant (subunit DΔD3) was co-expressed with subunit L(his) and subjected to the same purification procedure as was used for wild-type subunit D. The elution profile from the size-exclusion column for the sample containing subunit DΔD3 and subunit L(his) was similar to that observed for purification of the wild-type

D/L(his) heterodimer (Fig. 6). However, the DΔD3/L(his) heterodimer eluted at a greater elution volume, consistent with the expected smaller size of a the DΔD3/L(his) heterodimer (35 kDa) compared to wild-type heterodimer (40 kDa). The sizes of D subunits and the presence of subunit L(his) in each heterodimer was confirmed by SDS-PAGE (Fig. 6). The ability of subunit DΔD3 to co-purify with subunit L(his) and form a stable heterodimer reveals that domain 3 is not required for the interaction of subunit D with subunit L. Moreover, deletion of domain 3 from subunit D resulted in a heterodimer devoid of [4Fe-4S] clusters, as revealed by UV-visible spectroscopy and elemental analyses (Fig. 4 and Table 1). These results support that the eight cysteine residues in domain 3 are necessary for the binding of the two [4Fe-4S] clusters in *M. acetivorans* subunit D.

The formation of the M. acetivorans D/L heterodimer does not require disulfides in subunit D- *M. acetivorans* subunit D contains thirteen cysteine residues (Fig. 2). *M. acetivorans* subunit L has one cysteine residue. Each cysteine may be in the free reduced state (thiol), participate in disulfide bonding or serve to coordinate a cofactor (e.g. [4Fe-4S] cluster). The structure of the *S. solfataricus* D/L heterodimer revealed that each cysteine that is not a ligand to the [4Fe-4S] cluster participates in disulfide bonding, suggesting disulfides may be required for the formation and stability of the heterodimer (4). Thus, the number of thiols in purified *M. acetivorans* D/L(his) heterodimers was quantified using the thiol-specific reagent DTNB to infer the presence or absence of disulfides (18).

The purified D/L(his) heterodimers were first incubated in non-denaturing buffer containing DTNB under anaerobic conditions. Incubation of the D/L(his) heterodimer with DTNB resulted in the release of TNB that corresponds to fourteen thiols (Table 1), indicating that all fourteen cysteine residues are in the reduced state. The DΔD3/L(his) heterodimer reacted with DTNB under non-denaturing conditions to release TNB that corresponds to six thiols, consistent with the deletion of the eight cysteine residues of domain

8

3. There was no significant difference in the reactivity of each heterodimer with DTNB under denaturing conditions, indicating that each cysteine is readily accessible to DTNB in the folded state of the heterodimer. This result is consistent with the model showing that the domain 2 and 3 cysteine residues are relatively surface exposed within the heterodimer (Fig. 2). The cysteine residues of domain 2 of Rbp3 from yeast have been shown to coordinate a zinc ion, instead of participating in disulfide bonding. However, the reaction of C82, C85, C90, and C93 of domain 2 of *M. acetivorans* subunits D and subunit DΔD3 with DTNB under both non-denaturing and denaturing conditions suggests that these residues do not bind zinc or participate in disulfides under the examined conditions.

The quantitation of thiols in the D/L(his)-FeS heterodimer was more variable. Incubation of D/L(his)-FeS with DTNB under non-denaturing conditions produced TNB corresponding to sixteen thiols (Table 1). The number of thiols detected in the D/L(his)-FeS heterodimer is likely a combination of TNB produced by thiols and by sulfide released from the [4Fe-4S] clusters, as the reaction of one sulfide anion with DTNB yields two TNB anions (30). The addition of denaturant resulted in an increase in the number of thiols detected, consistent with an increase in sulfide released from the [4Fe-4S] clusters. These data indicate that the cysteine residues of the purified *M. acetivorans* D/L heterodimers are either in the thiol state or participate in coordination of the [4Fe-4S] clusters, indicating disulfides are not required for dimerization of *M. acetivorans* subunit D with subunit L.

The [4Fe-4S] clusters of M. acetivorans subunit D are oxygen-labile and affect the structural stability of the D/L heterodimer- The Fe-S clusters in proteins from methanogens are often oxygen-labile, including the [4Fe-4S] clusters in ferredoxin from *Methanosarcina* (28). The exposure of the D/L(his)-FeS heterodimer to air resulted in a time-dependent decrease in the absorbance at 390 nm, whereas no significant decrease at 390 nm was seen when the heterodimer was kept anaerobic (Fig. 7). To determine if destruction of the clusters due to oxygen exposure affects the stability of the D/L(his) heterodimer, oxygen-induced

structural changes were examined by size-exclusion chromatography. Each purified heterodimer was incubated under nitrogen or air for one hour and then subjected to size-exclusion chromatography under anaerobic conditions (Fig. 8A-C). For each sample, the fractions corresponding to heterodimer were collected, concentrated, and the UV-visible spectrum recorded (Fig. 8D-E). The elution profile of the non-reconstituted D/L(his) heterodimer following anaerobic incubation resulted in a major heterodimer peak and a minor peak which was consistent with a larger molecular weight aggregate of D/L(his). Exposure to oxygen resulted in a very slight increase in the population of the minor, non-heterodimer, species. Importantly, oxygen did not cause disassociation of subunit D and subunit L, as indicated by the lack of peaks that corresponded to D or L monomers. Compared to the collected, anaerobically-incubated heterodimer, a decrease in absorbance in the 300-420 nm range of the collected aerobically-incubated heterodimer was observed, consistent with some loss of the small amount of Fe-S cluster present in the non-reconstituted D/L(his) heterodimer.

The elution profile of the anaerobically-incubated D/L(his)-FeS heterodimer displayed a single heterodimer peak. While the non-reconstituted D/L(his) heterodimer exhibited some aggregation after anaerobic incubation, the lack of this aggregation by the D/L(his)-FeS suggests that the heterodimer is more stable (i.e. less structural heterogeneity) when both [4Fe-4S] clusters are present. In contrast, a substantial increase in the structural heterogeneity of the D/L(his)-FeS heterodimer was observed following aerobic incubation, as indicated by the appearance of two additional peaks in the elution profile (Fig. 8B). The increased structural heterogeneity is a result of oxygen-induced [4Fe-4S] cluster loss in the D/L(his)-FeS sample as revealed by the UV-visible spectrum of the collected heterodimer sample (Fig. 8E). The most likely explanation for the increased aggregation observed in the D/L(his)-FeS heterodimer, compared to the D/L(his) heterodimer, upon oxygen exposure is due to Fe-catalyzed production of reactive oxygen species leading to amino acid oxidation and protein aggregation. The presence of only a

9

heterodimer peak in the elution profile of both anaerobically-incubated and aerobically-incubated DΔD3/L(his) heterodimer, demonstrates that domain 3 is involved in the formation of the D/L(his) aggregates. These results suggest that the presence or absence of domain 3, along with the [4Fe-4S] clusters affect the structural stability of the D/L heterodimer. Overall, these data support that the presence of both [4Fe-4S] clusters are important for the integrity of domain 3 and serve to stabilize the D/L heterodimer.

Domain 3 of subunit D is not required for the formation of the D/L heterodimer within M. acetivorans- Co-purification of subunit DΔD3 with subunit L(his) after co-expression in *E. coli*, along with the complete lack of domain 3 in subunit D from all members of the *Methanococcales*, indicate that domain 3 of subunit D is not required for the formation of the D/L heterodimer within *M. acetivorans*. To test this hypothesis, two merodiploid strains of *M. acetivorans* were constructed. In addition to expressing native subunit D, these strains contain a second *rpoD* gene which encodes an N-terminally His-tagged subunit D and is under the control of a tetracycline-dependent promoter. Strain DJL30 expresses His-subunit D (His-D) and strain DJL31 expresses His-subunit DΔD3 (His-DΔD3). Importantly, subunit L was not tagged or over-expressed in these strains. Western blot analysis with anti-D/L antibodies of lysates from induced DJL30 cells did not reveal an increase in the concentration of subunit D, when compared to uninduced cells (data not shown). The inability to detect an increase in the cellular levels of subunit D in the merodiploid His-D expression strain is likely due to the degradation of unassembled subunits by proteases, which has been seen in yeast (31). This result is consistent with His-D competing with native D for association with endogenous subunit L and assembly into RNAP, with unassembled His-D or D being degraded. Inducible expression was seen in the DJL31 strain where a smaller immunoreactive protein (His-DΔD3) was detected only when DJL31 cells were grown in the presence of tetracycline (data not shown). Strains DJL30 and DJL31 grown in the absence and presence of

tetracycline exhibit a similar growth rate and cell yield (data not shown), indicating the expression of subunit D containing an affinity tag or the presence of subunit DΔD3 is not detrimental to *M. acetivorans*.

To verify expression and to determine if His-D and His-DΔD3 can associate with native subunit L, clarified cell lysates from strains DJL30 and DJL31 grown in the presence or absence of tetracycline were used for Ni^{2+}-affinity purification. Imidazole eluates from the columns were analyzed by Western blot using anti-D/L antibodies. A band consistent with subunit D or DΔD3 was only detected in the eluate from lysate of cells grown in the presence of tetracycline (Fig. 9), consistent with inducible expression of His-D and His-DΔD3 in strains DJL30 and DJL31, respectively. Moreover, endogenous subunit L (untagged) co-purified with both subunit His-D and His-DΔD3, revealing that domain 3 of subunit D is not required for the formation of the D/L heterodimer within *M. acetivorans* (Fig. 9). The additional immunoreactive proteins in the eluates are degradation products of unassembled His-D and His-DΔD3, similar to the appearance of Rpb3 degradation products when affinity-tagged Rpb3 is expressed in yeast (31-33).

DISCUSSION

The results presented herein reveal the ability of subunit D of RNAP from *M. acetivorans* to bind two redox-active and oxygen-labile [4Fe-4S] clusters. Given that all archaeal species harboring group 1 subunit D are strictly anaerobic, similar to *M. acetivorans*, it is highly likely that all group 1 subunit D contain two [4Fe-4S] clusters. However, the presence of a group 1 subunit D is not a universal feature of strictly anaerobic Archaea. In fact, there is extensive diversity in the properties of subunit D within the five orders of methanogens, indicating that the [4Fe-4S] clusters are not essential to the function of RNAP in methanogens. The presence of one or two [4Fe-4S] clusters in subunit D of archaeal RNAP likely imparts some advantage to those species that have acquired or retained this feature within their RNAP. Other DNA processing and repair enzymes, including helicase, primase,

10

glycosylases and endonucleases, bind [4Fe-4S] clusters (34), indicating these cofactors are a common, but not universal, feature of DNA processing enzymes. In many of these enzymes the [4Fe-4S] cluster is important to the structural stability of the enzyme and serves to monitor the redox state of the cell and modulate enzyme activity. For example, the DNA damage-inducible protein DinG, a DNA helicase, contains a [4Fe-4S] cluster that regulates DinG helicase activity (35). The [4Fe-4S] clusters in RNAP may serve a similar role. Based on previous structure-function studies of bacterial α N-terminal domain (αNTD) (36,37), eukaryotic Rpb3 (32,38), and archaeal D of RNAPs (2), along with results obtained with *M. acetivorans* subunit D, a plausible function for RNAP clusters is to regulate the *de novo* assembly of RNAP or to modulate the post-assembly activity of RNAP. A proposed model for the possible role(s) of the [4Fe-4S] clusters in *M. acetivorans* subunit D is presented in Fig. 10.

Iron is used as a cofactor in numerous metabolic enzymes in virtually all organisms. This is especially true in anaerobes, including methanogens. Methanogens are predicted to contain the largest number of [4Fe-4S] proteins, many of which are oxygen-labile (39). Many enzymes directly involved in methanogenesis including hydrogenases, carbon monoxide dehydrogenase, and heterodisulfide reductase, contain Fe-S clusters (40,41). These enzymes are rapidly inactivated in the presence of oxygen due to the oxidation and/or destruction of the Fe-S clusters, resulting in a decrease in energy available for biosynthesis. Moreover, 2[4Fe-4S] ferredoxin is a key electron transfer protein that interacts with a number of redox partners, including carbon monoxide dehydrogenase (40). In *M. acetivorans* and other organisms, the [4Fe-4S] clusters in ferredoxin-like domain 3 of subunit D may impart the ability to directly integrate global gene expression with the metabolic state of the cell.

One plausible role for the [4Fe-4S] clusters is to regulate the assembly of RNAP in response to cellular conditions, which is supported by previous studies documenting archaeal subunit D, bacterial α subunit and eukaryotic Rpb3 as key subunits that initiate the assembly of RNAP (9,10,37,38). The D/α/Rpb3

subunits are not directly involved in binding of template DNA and synthesis of RNA. Instead, one function of these subunits is to serve as a scaffold for the assembly and proper interaction of the catalytic subunits. In bacteria, the assembly of RNAP is initiated by α subunit dimerization and is assembled in the following order: $\alpha_I + \alpha_{II} \rightarrow \alpha_{I/II} \rightarrow \alpha_{I/II}\beta \rightarrow \alpha_{I/II}\beta\beta' \rightarrow \alpha_{I/II}\beta\beta'\sigma$ (36). The determinants for α dimerization are located within the αNTD. The β and β' subunits comprise the catalytic core. The assembly of eukaryotic Pol II is initiated by Rpb3 dimerization with Rpb11, followed by addition of Rpb2 to form the assembly subcomplex Rpb2-Rpb3-Rpb11, analogous to $\alpha_{I/II}\beta$. The catalytic subunit Rpb1, and the auxiliary subunits Rpb4-10 and Rbp12 then assemble to form complete Pol II. Similarly, the assembly of archaeal RNAP is initiated by the formation of a heterodimer of subunits D and L, followed by the addition of subunits N and P, forming the DLNP assembly platform (42). A stable BDLNP subcomplex that is competent in DNA binding and transcription factor interaction has also been identified, indicating subunit B is likely added prior to the addition of the core A' and A" subunits and auxiliary HKFE subunits (10). Subunit B is split into two polypeptides (B' and B") in some Euryarchaeota, including *M. acetivorans* (42).

The ability to purify the *M. acetivorans* D/L heterodimer which lacks the [4Fe-4S] clusters reveals that the clusters are not required for initial D/L heterodimer formation. However, the presence and redox state of the [4Fe-4S] clusters in domain 3 of subunit D may influence the interaction of subunit D with additional assembly or catalytic subunits. Moreover, the instability of recombinant subunit D when expressed in the absence of subunit L indicates that subunit L serves to stabilize subunit D and that dimerization occurs prior to [4Fe-4S] cluster incorporation (Fig. 10). Based on the *S. solfataricus* RNAP structure and previous interaction studies with *Pyrococcus furious* RNAP, the D/L heterodimer directly contacts subunits B, N, and P (4,10). In particular, Domain 3 of *S. solfataricus* subunit D is in close proximity to subunit B (B' in *M. acetivorans* RNAP), indicating that the conformational state of Domain 3 could impact the interaction

between the D/L heterodimer and the B subunit. The lack of cluster incorporation or loss of incorporated clusters likely increases the flexibility of domain 3 which could prevent favorable interaction of the D/L heterodimer with subunits B, N and P (Fig. 10).

Because *M. acetivorans* is a strict anaerobe and exposure to oxygen shuts down metabolism (17,43), one possible mechanism to globally conserve energy in order to maintain critical functions during times of iron-depletion or oxidative stress would be to decrease production of RNA to minimum levels adequate for cellular maintenance. The lack of cluster incorporation, the oxidation of the clusters, or oxidative loss of incorporated clusters within domain 3 of subunit D may prevent the *de novo* assembly of RNAP. Thus, the [4Fe-4S] clusters in RNAP may be used to sense metabolic factors within the cell, such as iron/sulfur levels and intracellular redox state, which are influenced by environmental factors (e.g. nutrients and oxygen). The reduction potential and oxidative/reductive stability of the clusters is likely tuned to the metabolism of each particular species. For example, the single [4Fe-4S] cluster in *S. solfataricus* subunit D, an aerobic archaeon, is quite stable in air compared with the two [4Fe-4S] clusters in subunit D from *M. acetivorans*, a strict anaerobe. One possible explanation for this difference is the presence of the disulfide bond, instead of a second cluster, in domain 3 of *S. solfataricus* subunit D (4), which is absent from *M. acetivorans* subunit D. The disulfide may serve to stabilize the cluster in *S. solfataricus* subunit D, such that the cluster is only lost under more extreme oxidative conditions. In addition to preventing the assembly of RNAP, oxidation or loss of the clusters in assembled RNAP may induce dispersion and subsequent inactivation of RNAP.

An alternative function of the clusters may be to regulate RNAP activity, whereby the clusters serve as a recognition element necessary for optimal protein-protein interactions with general or gene-specific transcription factors. Importantly, subunit D is on the periphery of archaeal RNAP, as is Rpb3 on eukaryotic Pol II, in a position to interact with general or specific transcription factors (4,44). The α subunit of bacterial RNAP is also the primary subunit that interacts with specific transcription factors to regulate promoter-dependent gene expression in bacteria (36). Moreover, Rpb3 has been shown to directly interact with a number of transcription factors (45,46). An Rpb3 mutagenesis study in yeast identified Rpb3 mutants with a temperature-sensitive defect in activator-dependent transcription, indicating that Rpb3 contains determinants for interaction with transcription factors (47). More recently, a direct interaction of Rpb3 with the Med17 subunit of the Mediator complex was demonstrated using an *in vivo* cross-linking approach (48). Mediator is a large multi-subunit complex conserved in eukaryotes that is required for transcription of most Pol II-transcribed genes. Mediator also serves to link specific regulatory proteins with the Pol II transcription complex. Therefore, Rpb3 is important for assembly and the direct interaction with general and specific transcription factors. Proteins that interact with subunit D of archaeal RNAP have not been identified, but given the high degree of similarity to Rpb3 it is highly likely subunit D contains regions required for interaction with transcription factors.

In *M. acetivorans,* 2[4Fe-4S] cluster-containing domain 3 of subunit D may function as a recognition element for the interaction with regulatory proteins needed to recruit RNAP to specific promoters or to control transcription initiation rates. Furthermore, given the rapid loss of the [4Fe-4S] clusters in the purified D/L(FeS) heterodimer upon exposure to air, the clusters may be used to sense the redox state of the cell to direct changes in gene expression. However, there may be differences in the stability of the [4Fe-4S] clusters in fully assembled RNAP. For example, the [4Fe-4S] cluster in *S. solfataricus* RNAP was more recalcitrant to removal by chelators as compared to the [4Fe-4S] cluster in D/L heterodimer. As seen with other DNA-interacting proteins, changes in the redox state of the [4Fe-4S] clusters in *M. acetivorans* RNAP may be enough to induce structural changes in domain 3 that alter the affinity for interacting partners. Oxidized RNAP may be recruited to the promoters of genes involved in response to stress. To test this hypothesis it will be

12

necessary to purify *M. acetivorans* RNAP and compare the properties of the [4Fe-4S] clusters to those of clusters in the D/L heterodimer. It is possible the clusters affect both the assembly and activity of RNAP. For example, exposure of *M. acetivorans* to oxygen and loss of the clusters from the D/L heterodimer may prevent assembly and oxidation or loss of the clusters from RNAP may direct RNAP to the promoters of genes needed for cellular maintenance. Using the established *M. acetivorans* genetic system, combined with *in vitro* approaches, it will be possible to test both the assembly and activity function of the [4Fe-4S] clusters. For example, the ability to generate the *M. acetivorans* strain capable of expressing subunit DΔD3 without a negative phenotype, indicates it will be possible to use this mutant to determine subunit D interacting partners which are dependent on Domain 3.

Conclusions-Our results from a survey of RNAP subunit D from sequenced Archaea reveal extensive diversity in the cysteine content and number of [4Fe-4S] cluster motifs, dividing archaeal RNAP into six distinct groups. Subunit D from species of an individual order typically falls within a single group, indicating that subunit D may be used as an additional marker for phylogenetic analyses. For example, all members of the Methanosarcinales encode a group 1 subunit D, whereas all Methanococcales encode group 6 subunit D. We have also demonstrated that subunit D from *M. acetivorans* is capable of binding two redox-active and oxygen-labile [4Fe-4S] clusters. Data obtained from recombinant studies reveal that the clusters and Domain 3 are not required for the formation of the D/L heterodimer, which was supported by *in vivo* studies revealing that domain 3 is not required for D/L heterodimer formation within *M. acetivorans*. Overall, these results suggest the clusters are not essential to RNAP, consistent with a regulatory role. Given the extreme sensitivity of the clusters to oxygen and the cluster-induced structural changes of the D/L heterodimer, a potential function is in the redox-dependent regulation of RNAP assembly and/or activity.

REFERENCES

1. Ebright, R. H. (2000) *J. Mol. Biol.* **304**, 687-698
2. Werner, F. (2008) *Trends Microbiol* **16**, 247-250
3. Haag, J. R., and Pikaard, C. S. (2011) *Nat. Rev. Mol. Cell. Biol.* **12**, 483-492
4. Hirata, A., Klein, B. J., and Murakami, K. S. (2008) *Nature* **451**, 851-854
5. Korkhin, Y., Unligil, U. M., Littlefield, O., Nelson, P. J., Stuart, D. I., Sigler, P. B., Bell, S. D., and Abrescia, N. G. (2009) *PLoS Biol.* **7**, e102
6. Kusser, A. G., Bertero, M. G., Naji, S., Becker, T., Thomm, M., Beckmann, R., and Cramer, P. (2008) *J. Mol. Biol.* **376**, 303-307
7. Johnson, D. C., Dean, D. R., Smith, A. D., and Johnson, M. K. (2005) *Annu. Rev. Biochem.* **74**, 247-281
8. Hirata, A., and Murakami, K. S. (2009) *Curr. Opin. Struct. Biol.* **19**, 724-731
9. Eloranta, J. J., Kato, A., Teng, M. S., and Weinzierl, R. O. (1998) *Nucleic Acids Res.* **26**, 5562-5567
10. Goede, B., Naji, S., von Kampen, O., Ilg, K., and Thomm, M. (2006) *J. Biol. Chem.* **281**, 30581-30592
11. Spahr, H., Calero, G., Bushnell, D. A., and Kornberg, R. D. (2009) *Proc. Natl. Acad. Sc.i USA* **106**, 9185-9190
12. Arnold, K., Bordoli, L., Kopp, J., and Schwede, T. (2006) *Bioinformatics* **22**, 195-201
13. Emsley, P., and Cowtan, K. (2004) *Acta. Crystallogr. D. Biol. Crystallogr.* **60**, 2126-2132

14.   Takahashi, Y., and Nakamura, M. (1999) *J. Biochem.* **126**, 917-926
15.   Cruz, F., and Ferry, J. G. (2006) *Biochim. Biophys. Acta.* **1760**, 858-864
16.   Bradford, M. M. (1976) *Anal. Biochem.* **72**, 248-254
17.   Lessner, D. J., and Ferry, J. G. (2007) *J. Bacteriol.* **189**, 7475-7484
18.   Ellman, G. L. (1959) *Arch. Biochem. Biophys.* **82**, 70-77
19.   Guss, A. M., Rother, M., Zhang, J. K., Kulkarni, G., and Metcalf, W. W. (2008) *Archaea* **2**, 193-203
20.   Metcalf, W. W., Zhang, J. K., Apolinario, E., Sowers, K. R., and Wolfe, R. S. (1997) *Proc. Natl. Acad. Sc.i USA* **94**, 2626-2631
21.   Sowers, K. R., Boone, J. E., and Gunsalus, R. P. (1993) *Appl. Environ. Microbiol.* **59**, 3832-3839
22.   Zinder, S. (1993) Physiological ecology of methanogens. in *Methanogenesis* (Ferry, J. G. ed.), Chapman and Hall, New York, NY. pp 128-206
23.   Galagan, J. E., Nusbaum, C., Roy, A., Endrizzi, M. G., Macdonald, P., FitzHugh, W., Calvo, S., Engels, R., Smirnov, S., Atnoor, D., Brown, A., Allen, N., Naylor, J., Stange-Thomann, N., DeArellano, K., Johnson, R., Linton, L., McEwan, P., McKernan, K., Talamas, J., Tirrell, A., Ye, W., Zimmer, A., Barber, R. D., Cann, I., Graham, D. E., Grahame, D. A., Guss, A. M., Hedderich, R., Ingram-Smith, C., Kuettner, H. C., Krzycki, J. A., Leigh, J. A., Li, W., Liu, J., Mukhopadhyay, B., Reeve, J. N., Smith, K., Springer, T. A., Umayam, L. A., White, O., White, R. H., Conway de Macario, E., Ferry, J. G., Jarrell, K. F., Jing, H., Macario, A. J., Paulsen, I., Pritchett, M., Sowers, K. R., Swanson, R. V., Zinder, S. H., Lander, E., Metcalf, W. W., and Birren, B. (2002) *Genome. Res.* **12**, 532-542
24.   Nakamura, M., Saeki, K., and Takahashi, Y. (1999) *J. Biochem.* **126**, 10-18
25.   Sweeney, W. V., and Rabinowitz, J. C. (1980) *Annu. Rev. Biochem.* **49**, 139-161
26.   Terlesky, K. C., and Ferry, J. G. (1988) *J. Biol. Chem.* **263**, 4080-4082
27.   Terlesky, K. C., and Ferry, J. G. (1988) *J. Biol. Chem.* **263**, 4075-4079
28.   Clements, A. P., Kilpatrick, L., Lu, W. P., Ragsdale, S. W., and Ferry, J. G. (1994) *J. Bacteriol.* **176**, 2689-2693
29.   Prince, R. C., and Adams, M. W. (1987) *J. Biol. Chem.* **262**, 5125-5128
30.   Crack, J. C., Green, J., Le Brun, N. E., and Thomson, A. J. (2006) *J Biol Chem* **281**, 18909-18913
31.   Mitobe, J., Mitsuzawa, H., and Ishihama, A. (2001) *Curr. Genet.* **39**, 210-221
32.   Kimura, M., and Ishihama, A. (2000) *Nucleic Acids Res.* **28**, 952-959
33.   Svetlov, V., Nolan, K., and Burgess, R. R. (1998) *J. Biol. Chem.* **273**, 10827-10830
34.   Genereux, J. C., Boal, A. K., and Barton, J. K. (2010) *J. Am. Chem. Soc.* **132**, 891-905
35.   Ren, B., Duan, X., and Ding, H. (2009) *J. Biol. Chem.* **284**, 4829-4835
36.   Ebright, R. H., and Busby, S. (1995) *Curr. Opin. Genet. Dev.* **5**, 197-203
37.   Ishihama, A. (1981) *Adv. Biophys.* **14**, 1-35
38.   Kimura, M., Ishiguro, A., and Ishihama, A. (1997) *J. Biol. Chem.* **272**, 25851-25855
39.   Major, T. A., Burd, H., and Whitman, W. B. (2004) *FEMS Microbiol. Lett.* **239**, 117-123
40.   Ferry, J. G. (2003) One-carbon metabolism in methanogenic anaerobes. in *Biochemistry and Physiology of Anaerobic Bacteria* (Ljungdahl, L. G., Adams, M. W., Barton, L. L., Ferry, J. G., and Johnson, M. K. eds.), Springer-Verlag, New York. pp 143-156
41.   Lessner, D. (2009) Methanogenesis: Biochemistry. in *Encyclopedia of Life Sciences*, Nature Publishing Group

42. Werner, F. (2007) *Mol. Microbiol.* **65**, 1395-1404
43. Brioukhanov, A. L., Netrusov, A. I., and Eggen, R. I. (2006) *Microbiology* **152**, 1671-1677
44. Cramer, P., Bushnell, D. A., and Kornberg, R. D. (2001) *Science* **292**, 1863-1876
45. De Angelis, R., Iezzi, S., Bruno, T., Corbi, N., Di Padova, M., Floridi, A., Fanciulli, M., and Passananti, C. (2003) *FEBS Lett.* **547**, 15-19
46. Oufattole, M., Lin, S. W., Liu, B., Mascarenhas, D., Cohen, P., and Rodgers, B. D. (2006) *Endocrinology* **147**, 2138-2146
47. Tan, Q., Linask, K. L., Ebright, R. H., and Woychik, N. A. (2000) *Genes Dev.* **14**, 339-348
48. Soutourina, J., Wydau, S., Ambroise, Y., Boschiero, C., and Werner, M. *Science* **331**, 1451-1454

FOOTNOTES

[1]To whom correspondence may be addressed: Department of Biological Sciences, University of Arkansas, Fayetteville, AR, USA, Tel.: (479) 575-2239; Fax: (479) 575-4010; E-mail: dlessner@uark.edu
[2]Department of Materials Science and Biotechnology, Ehime University, Bunkyo 3, Matusyama, Japan
[3]Department of Chemistry and Biochemistry, Auburn University, Auburn, Alabama, 36849

[4]The abbreviations used are: RNAP, RNA polymerase; DΔD3, subunit D deleted of domain 3; His, histidine tag; EPR, electron paramagnetic resonance; DTNB, dithionitrobenzoate; TNB, thionitrobenzoate; D/L(his), purified D/L heterodimer; D/L(his)-FeS, purified D/L heterodimer reconstituted with Fe/S; DΔD3/L(his), purified DΔD3/L heterodimer; His-D, six-histidine tagged subunit D; His-DΔD3, six-histidine tagged subunit DΔD3; αNTD, bacterial RNAP α N-terminal domain

Table 1. Comparison of the properties of the *M. acetivorans* D/L(his), D/L(his)-FeS, and DΔD3/L(his) heterodimers.

Heterodimer	A_{390}/A_{280}	ε_{390} (mM^{-1} cm^{-1})	Iron[a]	Sulfide[b]	Thiol[c]	Thiol[d] (denatured)
D/L(his)	0.06	2.2 ± 0.08	1.1 ± 0.1	1.1 ± 0.05	13.8 ± 0.4	14.5 ± 0.7
D/L(his)-FeS	0.50	33.2 ± 0.6	8.3 ± 0.2	7.7 ± 0.8	16.2 ± 0.3	21.5 ± 1.6
DΔD3/L(his)	0.01	0.2 ± 0.01	ND	ND	5.9 ± 0.7	5.4 ± 1.5

[a] nmol iron/nmol of DL heterodimer
[b] nmol acid-labile sulfide/nmol of DL heterodimer
[c] nmol thiols/nmol of DL heterodimer
[d] measured in buffer containing 6M guanidine-HCl
ND: not determined

FIGURE LEGENDS

FIGURE 1. Domain architecture and diversity of cysteine residue content of subunit D of archaeal RNAP. A) Domain architecture and cysteine content of subunit D from *Sulfolobus solfataricus* (Ss) (4). The regions comprising domains 1, 2 and 3 are indicated and shaded differently. The cysteine residues that function as ligands to a [4Fe-4S] cluster are indicated by 4Fe-4S. Cysteine residues documented to participate in disulfide bonds are indicated by dotted lines. B) Diagram depicting the six distinct groups of archaeal subunit D based on the number of complete or partial [4Fe-4S] cluster motifs within domain 3. The domain architecture is the same as depicted in panel A. The two [4Fe-4S] cluster motifs in group 1 subunit D are labeled #1 and #2, with #1 corresponding to the single [4Fe-4S] cluster motif in *S. solfataricus* Subunit D. Representative members of each group are shown: Ma, *Methanosarcina acetivorans;* Sa = *Sulfolobus acidocaldarius;* Ih = *Ignicoccus hospitalis;* Pi = *Pyrobaculum islandicum*; Hs = *Halobacterium salinarum*; Mr = *Methanocaldococcus jannaschii.*

FIGURE 2. Domain 3 of subunit D of RNAP from *M. acetivorans* is predicted to bind two [4Fe-4S] clusters similar to 2[4Fe-4S] cluster ferredoxin. A) Schematic of the domain architecture of *M. acetivorans* subunit D including an amino acid alignment of Domain 3 to 2[4Fe-4S] cluster ferredoxin (MA0431) from *M. acetivorans*. Conserved residues are indicated by an asterisk including the cysteine residues postulated to bind the two [4Fe-4S] clusters. B) Homology model of the heterodimer of *M. acetivorans* subunit D (red) and subunit L (yellow) D/L heterodimer. The two [4Fe-4S] clusters in domain 3 are represented by sphere model. C) Close-up view of domain 3 of subunit D showing putative cysteine ligands to each [4Fe-4S] cluster. The two [4Fe-4S] clusters in domain 3 are represented in stick model.

FIGURE 3. Purification of recombinant *M. acetivorans* D/L(his) and D/L(his)-FeS heterodimers. A) Anaerobic size-exclusion chromatography of eluate (~50 mg of total protein) from Ni^{2+}-affinity chromatography of *E. coli* cell lysate containing *M. acetivorans* subunit L(his) and subunit D. B) Same as panel A, except that the eluate was reconstituted with iron and sulfide prior to loading onto the size-exclusion column (see Materials and Methods for details). For each purification, samples from fractions containing peaks 1, 2, and 3 were analyzed by SDS-PAGE as indicated. The asterisk indicates the peak that is consistent with a the molecular weight of a D/L(his) heterodimer (40.2 kDa).

FIGURE 4. UV-visible spectra of purified D/L(his), D/L(his)-FeS, and DΔD3/L(his) heterodimers. Line a, D/L(his) (67.5 µM); line b, D/L(his)-FeS (13.5 µM); line c, DΔD3/L(his) (67.5 µM). The inset shows the D/L(his)-FeS heterodimer before (solid line) and after (dashed line) the addition of sodium dithionite (10 mM).

FIGURE 5. EPR spectra of the D/L(his)-FeS heterodimer before (a) and after the addition of dithionite (b). The sample contained 150 µM D/L(his)-FeS in 50 mM HEPES, 50 mM NaCl, pH 7.5. EPR conditions: microwave frequency, 9.385 GHz; microwave power incident to the cavity, 2.0 mW; field modulation frequency, 100 kHz; microwave amplitude, 0.6 mT; temperature 8 K.

FIGURE 6. Co-purification of *M. acetivorans* subunit DΔD3 with subunit L(his) after co-expression in *E. coli*. A) Anaerobic size-exclusion chromatography of eluate (~50 mg of total protein) from Ni^{2+}-affinity chromatography of *E. coli* cell lysate containing *M. acetivorans* subunits L(his) and DΔD3. The asterisk indicates the peak which is consistent with a the molecular weight of a heterodimer of DΔD3/L(his) (34.8 kDa). B) SDS-PAGE analysis of the purified D/L(his) (lane 1) and DΔD3/L(his) (lane

16

2) heterodimers, confirming the smaller molecular weight of DΔD3 (23.3 kDa) compared to D (28.7 kDa).

FIGURE 7. Effect of oxygen on the stability of the [4Fe-4S] clusters in purified D/L(his)-FeS heterodimer. The loss of the [4Fe-4S] clusters in purified D/L(his)-FeS (20 μM) incubated under N_2 or in air in 50 mM HEPES, 50 mM NaCl, pH 7.5 was monitored by measuring A_{390} over time.

FIGURE 8. Effect of oxygen on the stability of the D/L(his), D/L(his)-FeS, and DΔD3/L(his) heterodimers. Each heterodimer was incubated anaerobically or aerobically in 50 mM HEPES, 50 mM NaCl, pH 7.5 and analyzed by size-exclusion chromatography under anaerobic conditions using a running buffer of 50 mM HEPES, pH 7.5, 150 mM NaCl. Elution profiles of each heterodimer after anaerobic (solid line) or aerobic incubation (dashed line) are shown in panels A-C. Panel A: D/L(his), 1.1 mg each; panel B: D/L(his)-FeS, 0.8 mg each; panel C: DΔD3/L(his), 1.5 mg each. For each elution profile an asterisk indicates the heterodimer peak and arrows indicate D/L(his) aggregates. The UV-visible spectra of concentrated fractions containing heterodimer from anaerobic samples (solid line) and aerobic samples (dashed line) are shown in panels D-F. Panel D: D/L(his), 26 μM each; panel E: D/L(his)-FeS, 10 μM each; panel F: DΔD3/L(his),18 μM each.

FIGURE 9. Co-purification of endogenous subunit L with His-tagged subunit D or subunit DΔD3 expressed within *M. acetivorans*. Western blot of a 15% SDS-PAGE gel with anti-D/L antibodies. Lane 1, recombinant D/L(his) heterodimer (50 ng); lane 2, recombinant DΔD3/L(his) heterodimer (150 ng); lane 3, imidazole eulate from a Ni^{2+}-agarose column loaded with cell lysate of DJL30 grown in the absence of tetracycline; lane 4, imidazole eluate from a Ni^{2+}-agarose column loaded with cell lysate of DJL30 grown in the presence of tetracycline; lane 5, imidazole eulate from a Ni^{2+}-agarose column loaded with cell lysate of DJL31 grown in the absence of tetracycline; lane 6, imidazole eulate from a Ni^{2+}-agarose column loaded with cell lysate of DJL31 grown in the presence of tetracycline. The asterisks indicate subunit His-D degradation products.

FIGURE 10. Model depicting the potential roles of the subunit D [4Fe-4S] clusters in modulating the assembly and/or activity of *M. acetivorans* RNAP. The three domains of subunit D are represented by 1, 2, and 3. A change in the reduction state of each [4Fe-4S] cluster is indicated by a circle versus a square. The dashed semi-circle arrow depicts the increased flexibility of domain 3 upon loss of the [4Fe-4S] clusters.
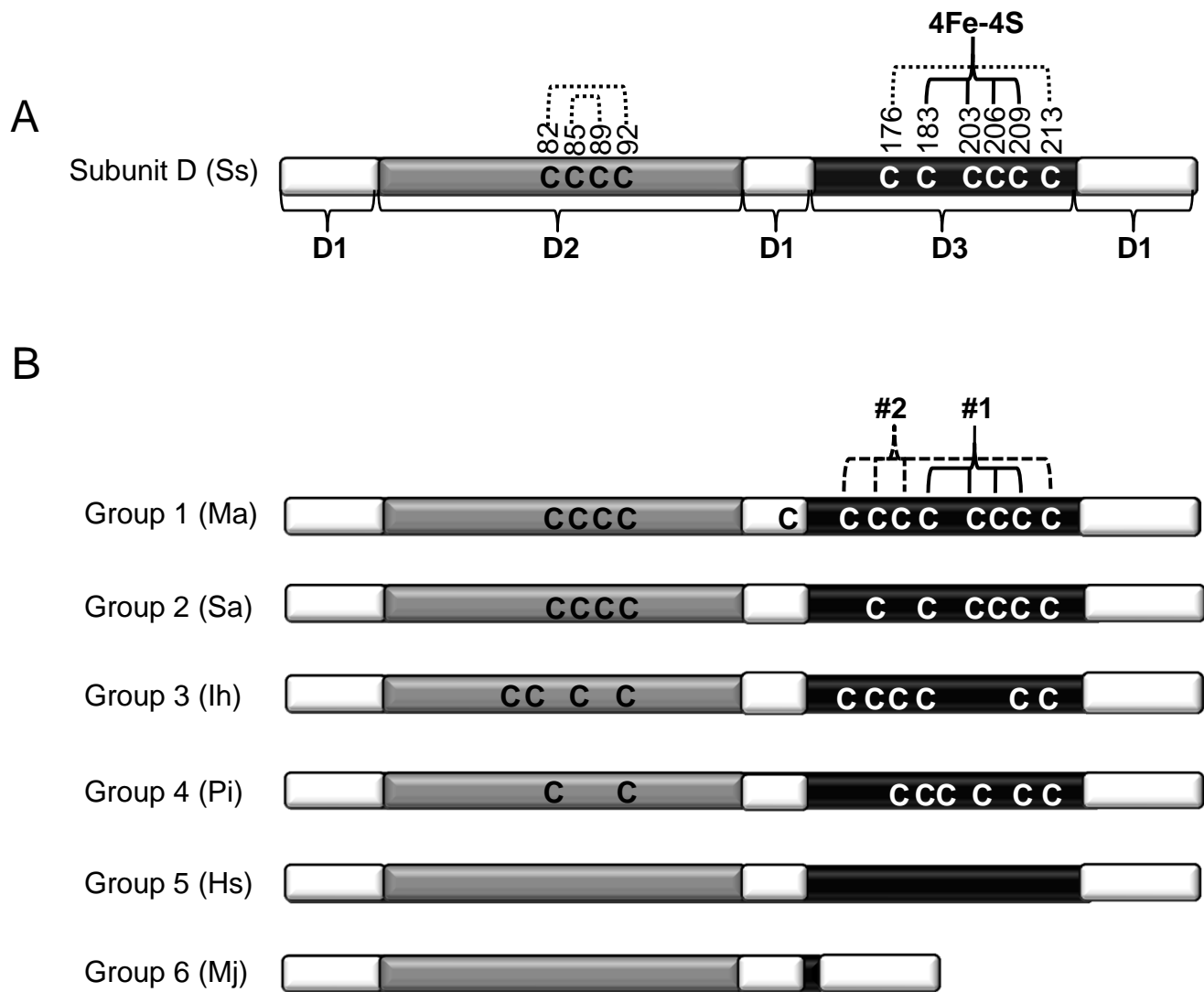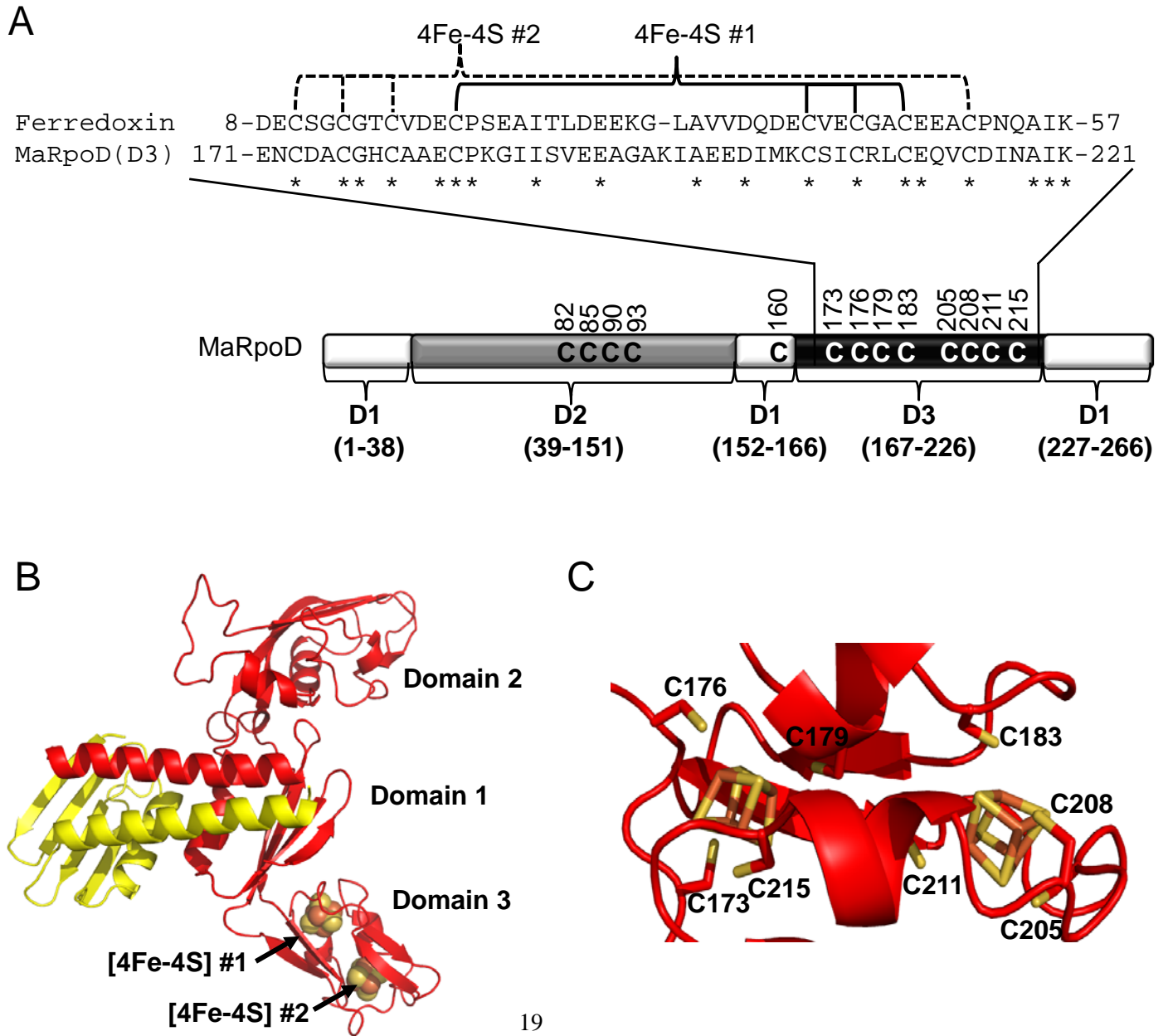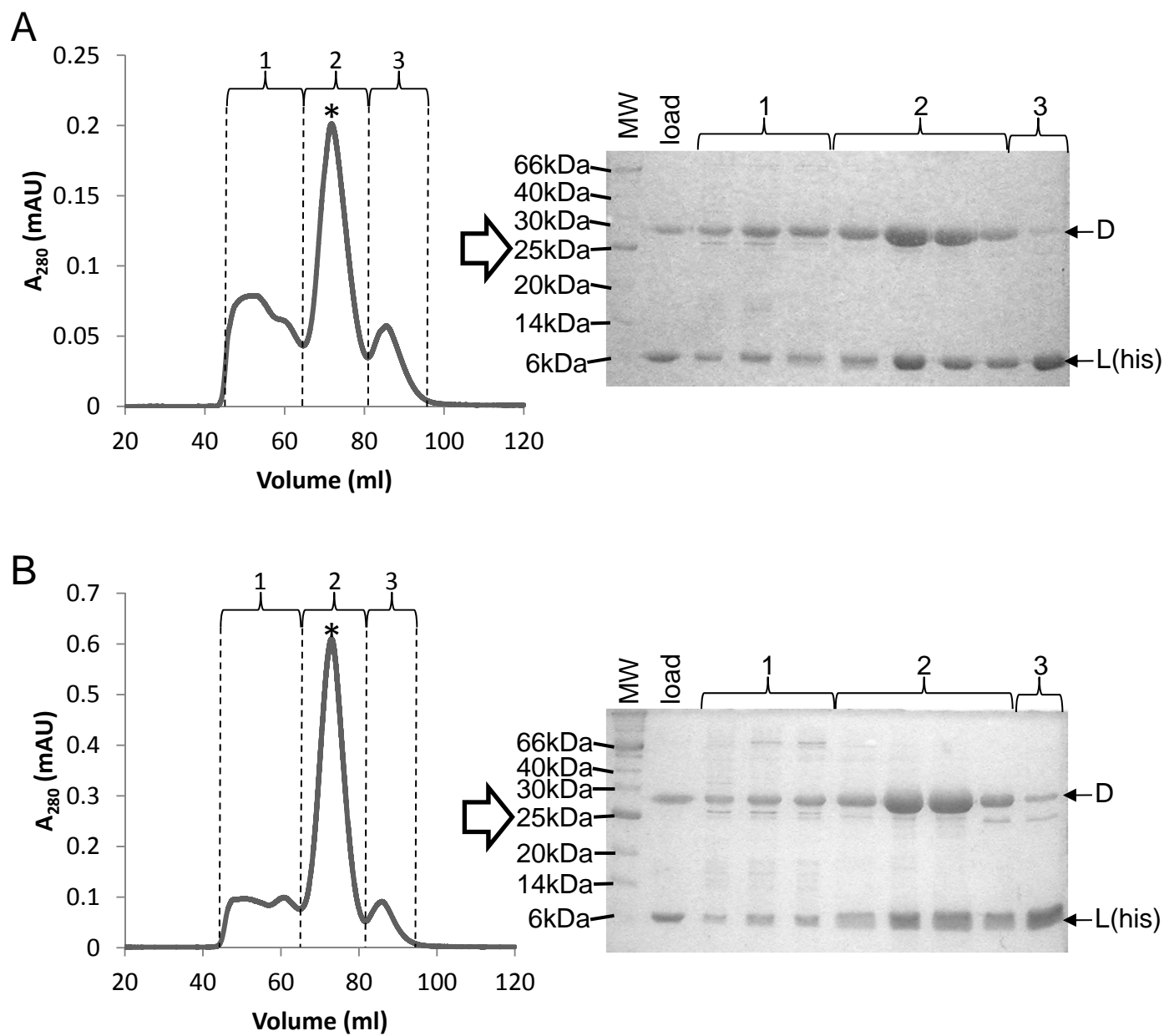
Figure 1

Figure 2

A


```
                           4Fe-4S #2            4Fe-4S #1

Ferredoxin    8-DECSGCGTCVDECPSEAITLDEEKG-LAVVDQDECVECGACEEACPNQAIK-57
MaRpoD(D3)  171-ENCDACGHCAAECPKGIISVEEAGAKIAEEDIMKCSICRLCEQVCDINAIK-221
                 *  ** *  ***    *     *      *   *    *   *   **  *   ***
```

MaRpoD

D1 (1-38)   D2 (39-151)   D1 (152-166)   D3 (167-226)   D1 (227-266)

B

Domain 2
Domain 1
Domain 3
[4Fe-4S] #1
[4Fe-4S] #2

C

C176
C179
C183
C208
C173
C215
C211
C205

19

Figure 3

Figure 4

Figure 5
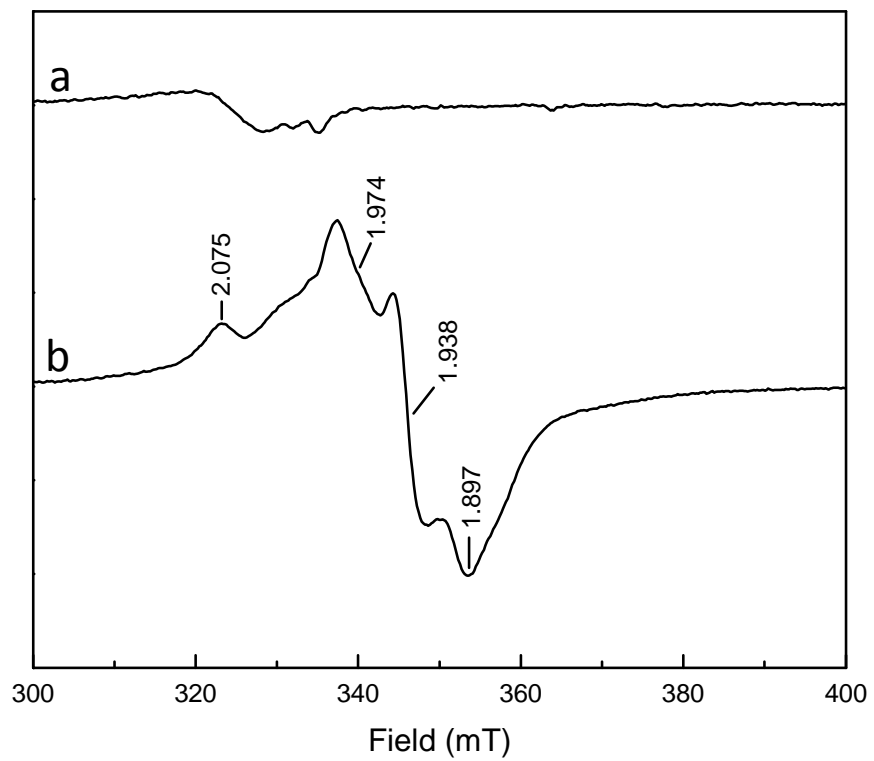
Figure 6
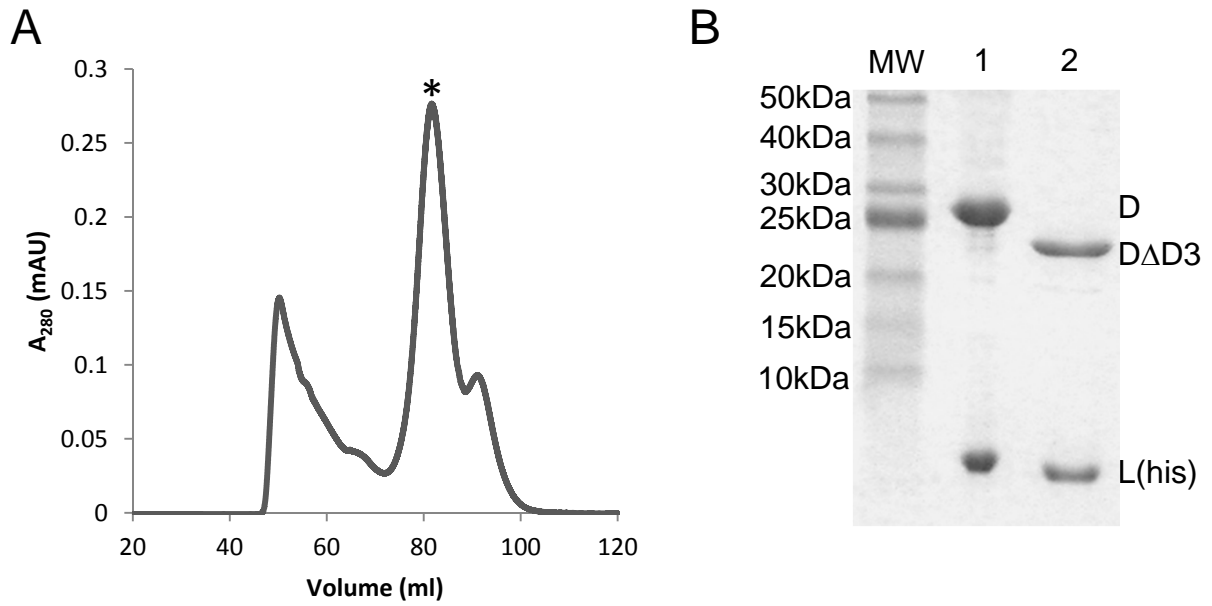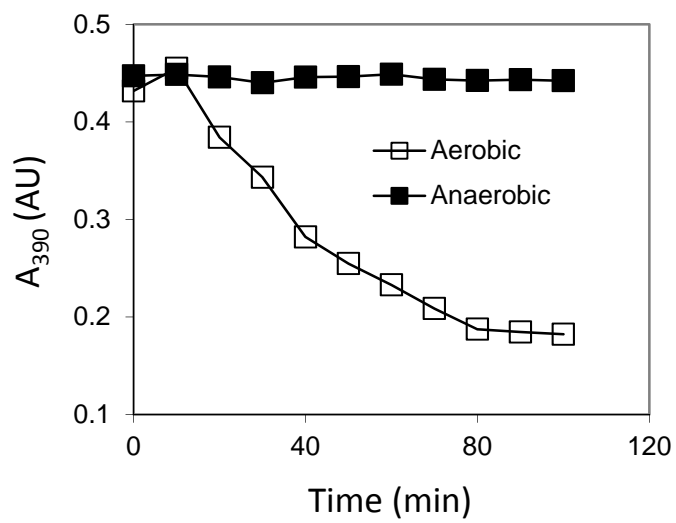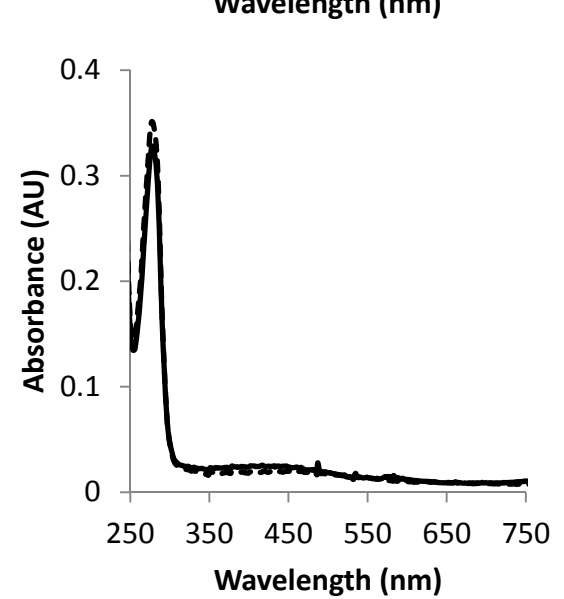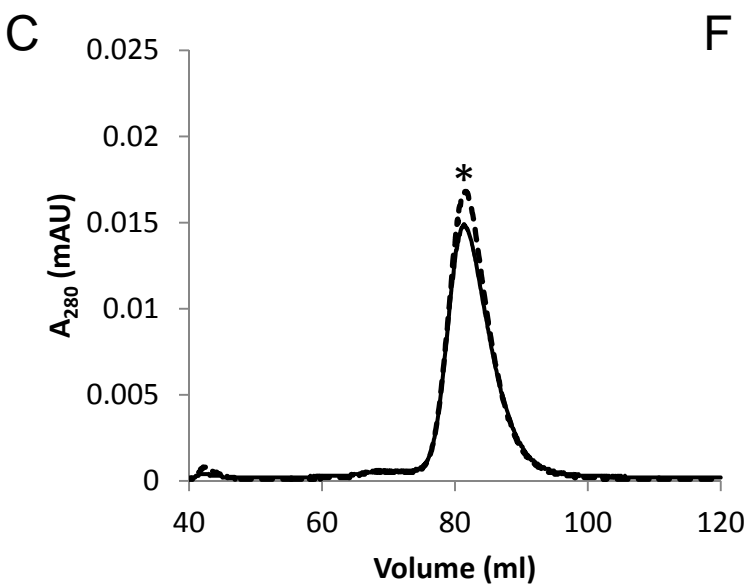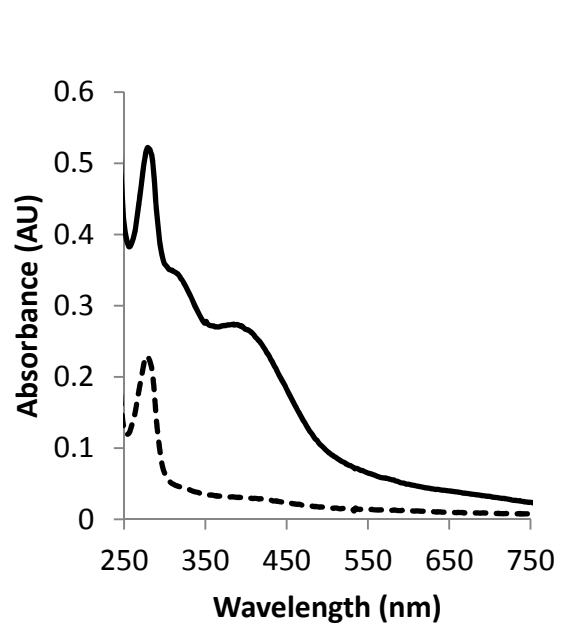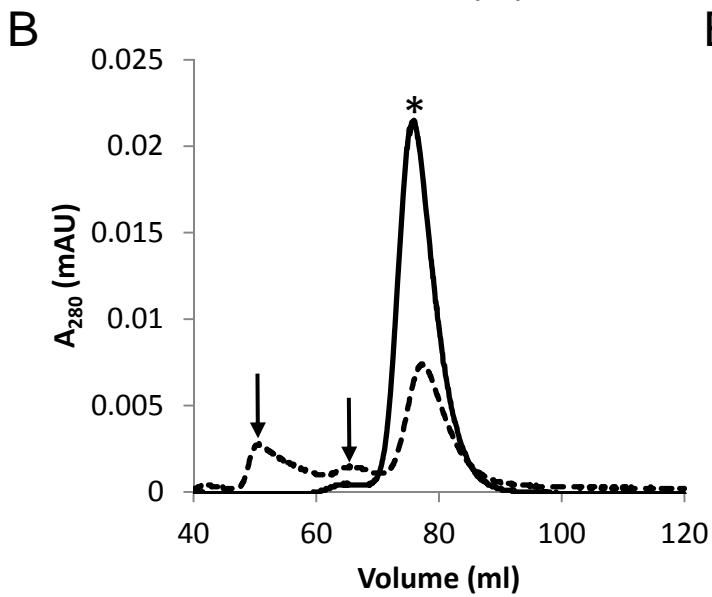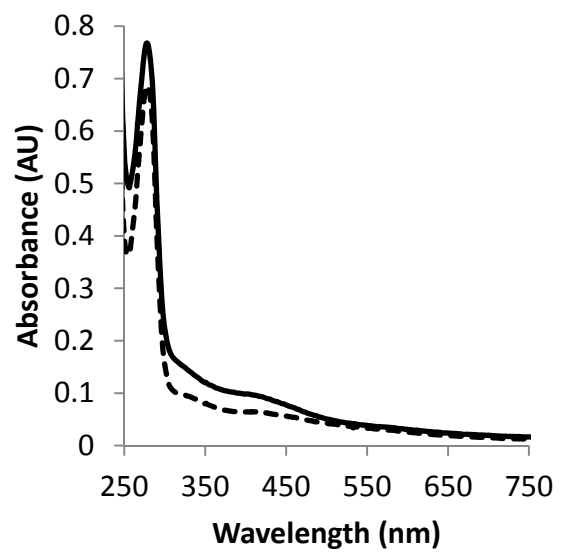
A

B

Figure 7

24

Figure **8**

Figure 9

Figure 10

The oxidation state or loss of the [4Fe-4S] clusters may affect interaction with additional subunits or transcription factors to regulate the assembly and/or activity or RNAP
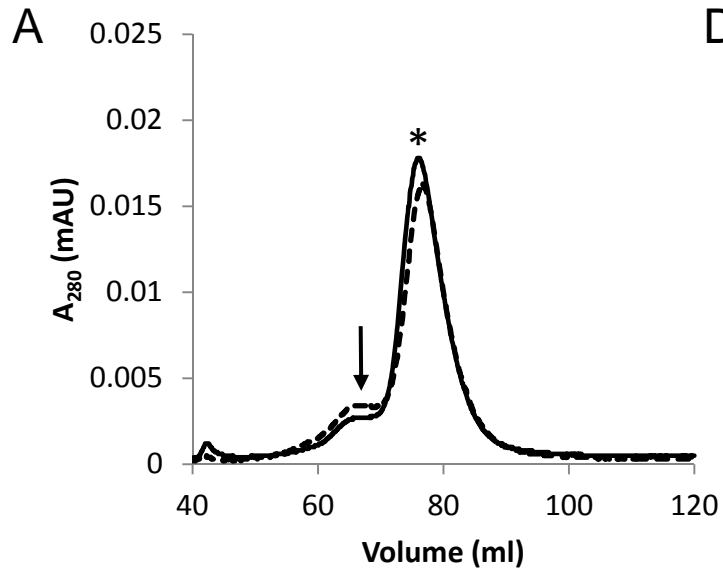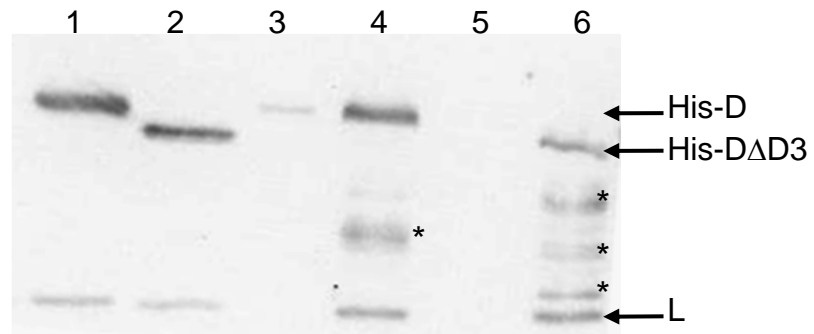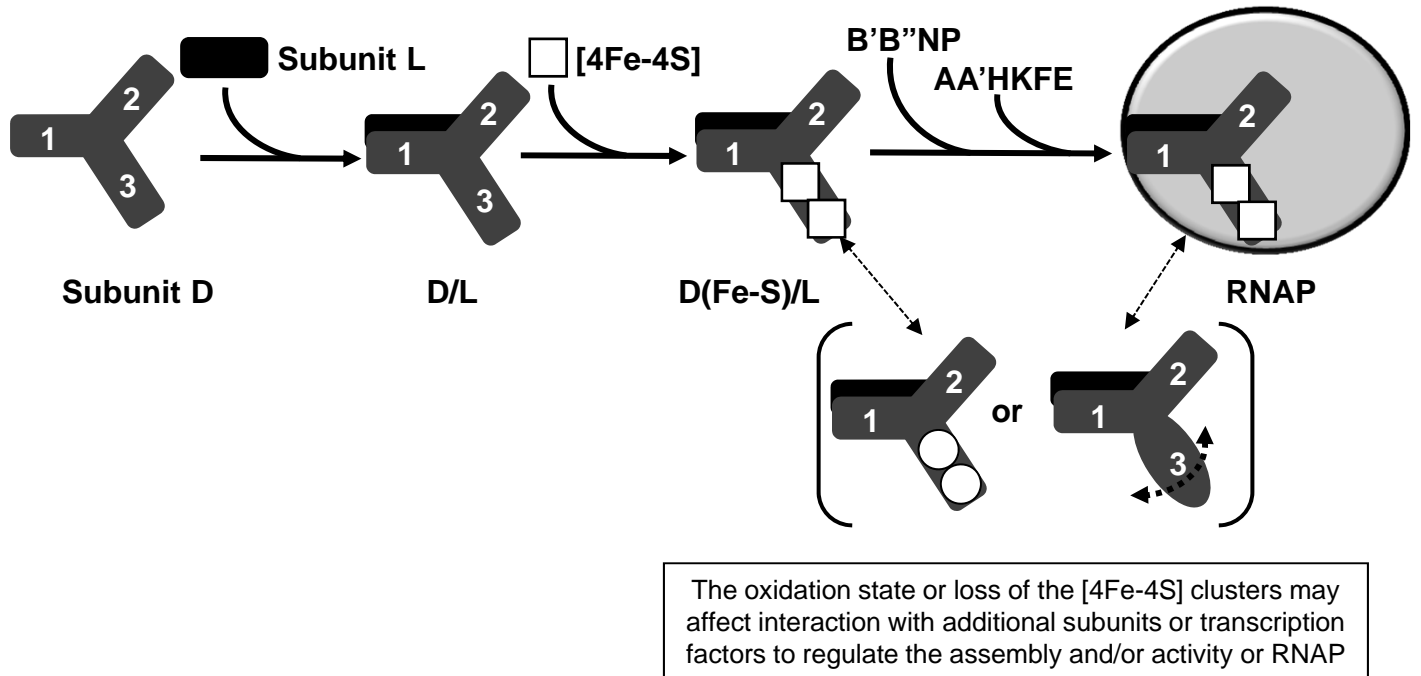
Subunit D of RNA polymerase from Methanosarcina acetivorans contains two oxygen-labile [4Fe-4S] clusters: implications for oxidant-dependent regulation of transcription

Faith H. Lessner, Matthew E. Jennings, Akira Hirata, Eduardus C. Duin and Daniel J. Lessner

Access the most updated version of this article at doi: 10.1074/jbc.M111.331199

Alerts:

- When this article is cited
- When a correction for this article is posted

Click here to choose from all of JBC's e-mail alerts

Supplemental material:
http://www.jbc.org/content/suppl/2012/03/28/M111.331199.DC1